

DOI: 10.1002/cphc.201300733

Polymeric Heterogeneous Catalysts of Transition-Metal Oxides: Surface Characterization, Physicomechanical Properties, and Catalytic Activity

Bui Dinh Nhi,* Renat Maratovich Akhmadullin, Alfiya Garipovna Akhmadullina, Yakov Dmitrievich Samuilov, and Svetlana Ivanova Aghajanian^[a]

We investigate the physicomechanical properties of polymeric heterogeneous catalysts of transition-metal oxides, specifically, the specific surface area, elongation at break, breaking strength, specific electrical resistance, and volume resistivity. Digital microscopy, Fourier-transform infrared spectroscopy, X-ray diffraction, scanning electron microscopy, and energy-dispersive analysis are used to study the surfaces of the catalysts. The experimental results show that polymeric heterogeneous catalysts of transition-metal oxides exhibit high stability and can maintain their catalytic activity under extreme reaction

conditions for long-term use. The oxidation mechanism of sulfur-containing compounds in the presence of polymeric heterogeneous catalysts of transition-metal oxides is confirmed. Microstructural characterization of the catalysts is performed by using X-ray computed tomography. The activity of various catalysts in the oxidation of sulfur-containing compounds is determined. We demonstrate the potential application of polymeric heterogeneous catalysts of transition-metal oxides in industrial wastewater treatment.

1. Introduction

The treatment of sulfurous alkaline waste containing toxic sulfide and hydrosulfide compounds is one of the major challenges faced by refineries and petrochemical plants. Chemical oxidation methods are most frequently used to treat these streams, whereby the sulfides react to form sulfates in air or pure oxygen.^[1,2] This reaction is very slow at atmospheric pressure and room temperature. The oxidation rate is accelerated in the presence of catalysts. Universal Oil Products, an American company, performs the catalytic oxidation of mercaptans in alkaline media in the presence of a catalyst, consisting mainly of sulfonated derivatives of a cobalt phthalocyanine complex, to remove much of the sulfur from petrol.^[3,4] This process is known as “merox”. Heterogeneous catalysts of transition metals combined with polymeric phthalocyanine have been applied for the oxidation of sulfur-containing compounds.^[5–8] Polymeric metal phthalocyanines and cobalt phthalocyanine sulfonates coordinately bound to polymers have been observed to be more effective than conventional cobalt phthalocyanine sulfonate catalysts.^[4,9] However, the synthesis of metal phthalocyanines is time consuming^[10–12] and cobalt phthalocyanine is too expensive for large-scale applications.^[13]

Currently, transition-metal oxides based on a polymer matrix are the main heterogeneous catalysts used in the oxidation of sulfide and hydrosulfide anions.^[14] Polymeric heterogeneous catalysts of transition-metal oxides exhibit high reactivity over

a wide range of oxidizable compound concentrations and pH levels, high mechanical strength, and good chemical and hydrolytic stability for three to five years. Polymer-based catalysts can be used under alkaline conditions at temperatures up to 100 °C and pressures up to 7.0 kg cm⁻².^[5,9] Many highly efficient systems have been developed for catalytic aerobic sulfide oxidation using rhenium-,^[15] palladium-,^[16] ruthenium-,^[17] and gold-based catalysts.^[18] However, these catalysts can be expensive, may hinder the purification of products, and are harmful to the environment. Only a few catalyst systems, such as those containing small amounts of inexpensive metal oxides, allow for the efficient aerobic oxidation of sulfides under severe conditions.^[19] However, a more robust and efficient catalyst system for the aerobic oxidation of sulfides under severe conditions has long been needed.

Our research was inspired by the observation of the activity of polymeric heterogeneous catalysts of transition-metal oxides and their mixtures in the oxidation of sulfur-containing compounds reported by Nhi et al.,^[9,20–24] who indicated that multicomponent catalysts exhibit high catalytic activity and identified the sulfide oxidation mechanism on the surface (external) of the catalysts. The researchers also investigated some of the factors that affect the oxidation rate. The surface characterization and physicomechanical properties of polymeric heterogeneous catalysts are reported herein.

[a] B. D. Nhi, Dr. R. M. Akhmadullin, Dr. A. G. Akhmadullina, Dr. Y. D. Samuilov, Dr. S. I. Aghajanian
Department of Technological Synthetic Rubber of Kazan
National Research and Technology University
420015, K. Marks St, Bldg 72. (Russian Federation)
E-mail: vietnamkz@yahoo.com

Experimental Section

Materials

All reagents were obtained from Kazpelen in the highest grade available and were used without further purification. During the experiments, the following oxides of metals with variable valencies were used: MnO_2 (Russia, GOST 4470-79), CuO (Russia, GOST 16539-79), NiO (Russia, GOST 4331-78), Cr_2O_3 (Russia, GOST 2912-79), cobalt oxide (II, III) (Russia, GOST 4467-79), and cobalt phthalocyanine (Russia, TU 6-07-1135-78). The polymer used was a high-molecular-weight polymer composed of polyethylene, known commercially as Kazpelen No. 15313-003. Stock sulfide solutions were created by dissolving sodium sulfide nonahydrate in deionized water and were used within 1 h of preparation to minimize losses through aerial oxidation. Deionized water was used in all experiments. All other solvents that were used were of analytical grade.

Catalyst Preparation

Laboratory samples of the heterogeneous catalysts were prepared by roll-mixing the catalytically reactive component (transition-metal oxides or phthalocyanine cobalt) with the molten polymer at 150°C until a uniform mass was obtained, after which, shavings with a thickness of 0.25 mm were formed (specific surface area of approximately $100\text{ cm}^2\text{g}^{-1}$). These catalysts could be prepared in the form of granules (particle size of $2\times 2\times 2\text{ mm}$) using the same equipment used to obtain carbon black concentrates or dye concentrates in polyethylene or polypropylene production. Packing elements could be prepared from the catalyst granules in casting machines.^[25] The metal-oxide content, expressed as wt% of metal oxide in the catalyst samples, was determined by using chemical analysis (in this work, the nomenclature CuO-5- indicates that the heterogeneous catalyst contained 5.0 wt% copper oxide). The catalyst was washed with distilled water for 10 h at 60°C before testing.

Experimental Procedures and Analytical Methods

Na_2S oxidation in aqueous NaOH solution was conducted in an air-bubbling vessel of an oxidation tower. Oxygen was fed into the reaction solution at 30 Lh^{-1} with an exact concentration of Na_2S in the presence of the catalytic agent. The solution inside the reactor was stirred at a speed of 1400 revmin^{-1} . The temperature of the reaction solution was maintained at 60°C with a thermally controlled magnetic mixer (Figure 1).

The concentration of Na_2S in the solution was measured by using the potentiometric titration method with an aqueous AgNO_3 solution.^[26] The concentration of Na_2SO_4 was determined by using spectrophotometry (SS1207UV, regime A, wavelength $\lambda = 450\text{ nm}$, path length $L = 50.0\text{ mm}$), and the concentrations of $\text{Na}_2\text{S}_2\text{O}_3$ and Na_2SO_3 , as well as the concentration of Na_2S , were determined by using iodometry.^[27]

Catalyst Characterization

Catalysts based on copper and manganese oxides (MnO_2 , CuO) were used for testing. The specific surface areas (S_{sp}) and pore volumes (V_{p}) of the samples were determined by using low-temperature N_2 adsorption (Quantachrome Autosorb iQ-MP universal analyzer, USA). S_{sp} was determined based on the surface area of a N_2 molecule (0.162 nm^2) and its density in the normal liquid state (0.808 g cm^{-3}), with a measurement accuracy of $S_{\text{sp}} \pm 3\%$. Adsorption isotherms were obtained at -196°C after degassing each

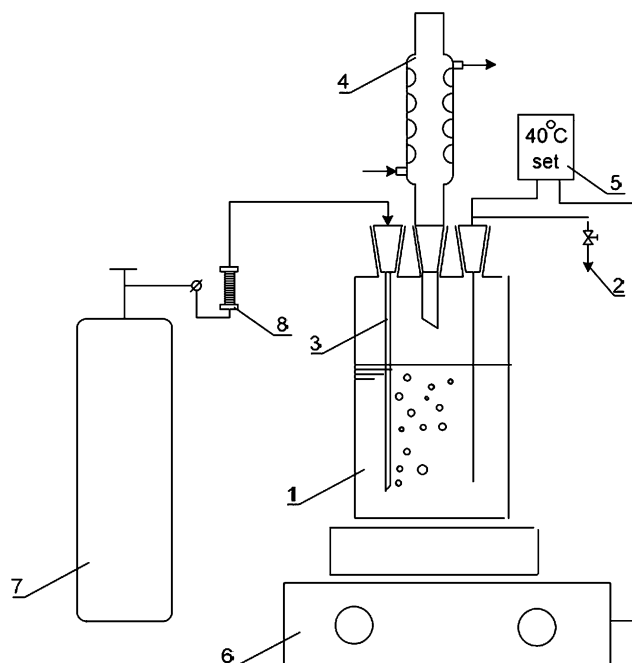


Figure 1. Oxidation tower apparatus: 1) 150 mL cylindrical glass vessel, 2) sampling, 3) gas supply tube, 4) condenser, 5) electronic temperature controller (Hei-Con), 6) magnetic stirrer (Hei-Standard Company Heildolf), 7) oxygen vessel, and 8) oxygen regulator.

sample at 500°C and a residual pressure of 0.013 Pa. V_{p} was determined by using the Brunauer–Emmett–Teller (BET) equation and the Barrett–Joyner–Halenda (BJH) method^[28] (measurement accuracy $V_{\text{p}} \pm 13\%$).

The samples were analyzed by using X-ray diffraction (XRD) with $\text{CuK}\alpha$ radiation at 40 kV and 40 mA (Philips Xpert, X-ray wavelength $\gamma = 0.15406\text{ nm}$) and a time constant of 0.5 s; a crystal graphite monochromator was used to identify the phases present (metals and transition-metal oxides).

2D and 3D X-ray-computed tomography images were analyzed to quantify the shape characteristics of the catalysts. These images were obtained by using the nanofocal tube of a GE Phoenix v|tome|x s240 industrial X-ray microtomography system at an accelerating voltage of 90 kV and a current of 170 mA. Data reconstruction software was used to create primary models of the X-ray images (projections). The image resolution was $4\text{ }\mu\text{m}$. VGStudio-MAX software (version 2.1) was used for 2D image and video analysis. All 3D models were built using AvizoFire software (version 7.1).

Scanning electron microscopy (SEM) images were obtained by using a Merlin Carl Zeiss auto-emission scanning electron microscope operated at an accelerating voltage of 5 keV. Samples were coated with a thin film of gold by using a sputtering device. To determine the actual composition of the catalysts, an AZtec X-MAX energy-dispersive spectroscopy (EDS) instrument was used. Elemental analysis was carried out at an accelerating voltage of 20 keV and a working range of 9 mm, thus minimizing experimental error. The probing depth was at least $1\text{ }\mu\text{m}$.

The physicomechanical properties (elongation at break and breaking strength) of the polymeric catalysts were investigated by using an Inspekt mini 3 kN universal tensile machine in accordance with

Table 1. Physicomechanical properties of synthesized catalysts.

Catalyst	Content [wt %]		S_{sp} [$\text{cm}^2 \text{g}^{-1}$]	Elongation at break [%]	Breaking strength [MPa]	Specific electrical resistance [$\times 10^{-12} \Omega$]	Volume resistivity [$\times 10^{-12} \Omega \text{m}$]
	MnO_2	CuO					
pure polyethylene	–	–	89	689.5	14.3	6.1	44.2
$\text{MnO}_2/\text{CuO-5}$	2.5	2.5	92	837.4	17.1	10.6	67.5
$\text{MnO}_2/\text{CuO-10}$	5	5	93	799	15.2	9.8	63.2
$\text{MnO}_2/\text{CuO-15}$	7.5	7.5	95	857.4	17.5	8.8	56.9
$\text{MnO}_2/\text{CuO-20}$	10	10	94	788.9	15.4	8.4	52.1

ASTM D412 and ISO 37 at a temperature of $20 \pm 2^\circ\text{C}$. The organic groups on the catalyst surface were characterized before and after three months of use through digital microscopy (Keyence-VH-Z500R) and Fourier-transform infrared spectroscopy (FTIR) (Infracum-FT-08). Spectra were obtained over a range of 400 to 7800 cm^{-1} at 220 V and a power level of 65 W . The specific electrical resistance and volume resistivity were determined by using an E 6-13 teraohmmeter.

2. Results and Discussion

Physicomechanical Properties of the Synthesized Catalysts

The physicomechanical properties of the polymeric heterogeneous catalysts are presented in Table 1. The results show that the S_{sp} of the catalysts did not change significantly as the concentration of the transition-metal oxides increased, which can, most likely, be attributed to the use of an appropriate catalyst preparation method. $\text{MnO}_2/\text{CuO-15}$, consisting of 7.5 wt% CuO, 7.5 wt% MnO_2 , and 85 wt% polyethylene, exhibited the highest S_{sp} ($95 \text{ cm}^2 \text{g}^{-1}$). The evaluation of the elongation at break and breaking strength of these catalysts showed that the transition-metal oxides could be blended with a polymeric material, and that they were well-distributed within the polymeric matrix. Therefore, the addition of transition-metal oxides to the polymeric matrix enhanced the stability of the structure of the polymeric heterogeneous catalysts; accordingly, the elongation at break and breaking strength increased with increasing concentration of the transition-metal oxides. $\text{MnO}_2/\text{CuO-15}$ also showed the highest elongation at break (857.4%) and breaking strength (17.5 MPa). It is well known that polyethylene is non-conductive and is predominantly ionic in character. The electrical conductivity of polyethylene increases with crystallization, but the ionic conductivity decreases.^[29,30] Thus, the specific electrical resistance and volume resistivity of the presented catalysts increased with the addition of transition-metal oxides to the polymeric matrix, but decreased with the concentration of transition-metal oxides.

Morphology and Elemental Analysis of Polymeric Catalyst Surface

The surface of the $\text{MnO}_2-10/\text{CuO-10}$ catalyst, consisting of 10 wt% CuO, 10 wt% MnO_2 , and 80 wt% polyethylene, was investigated by using digital microscopy (Figure 2) and FTIR spectroscopy (Figure 3). The catalyst surface remained unchanged after three months of use, under relatively severe reaction conditions (60°C , 5.0% alkaline concentration, and

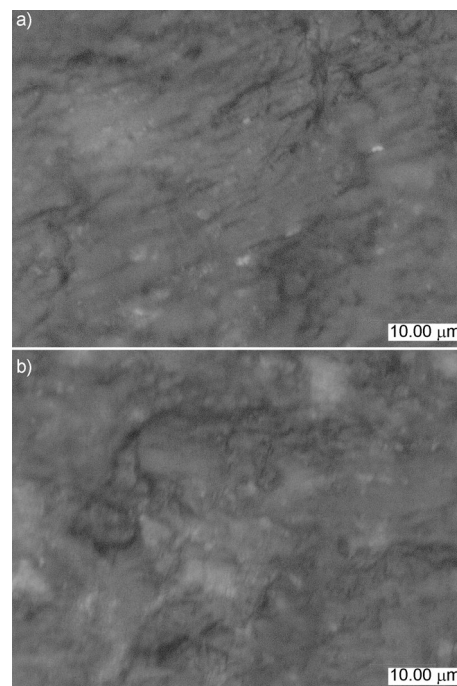


Figure 2. Digital microscopy images of the $\text{MnO}_2-10/\text{CuO-10}$ catalyst surface a) before reaction and b) after three months of use.

$1400 \text{ rev min}^{-1}$ solution rotational speed). The presented FTIR spectra show only the absorption bands of polyethylene, such as those indicating the valence vibrations of the C–H bonds of $-\text{CH}_2$ groups at $2870\text{--}2845 \text{ cm}^{-1}$, the deformation vibrations in $-\text{CH}_2$ groups at $1480\text{--}1440 \text{ cm}^{-1}$, and variations of the carbon skeletal $(\text{CH}_2)_x$ fragments at $720\text{--}740 \text{ cm}^{-1}$. Long-term operation was not accompanied by the appearance of any appreciable amounts of oxygen-containing groups (e.g. alcohol, carbonyl, carboxyl) in the polymeric matrix.

XRD analysis was performed to study the crystalline structure of the polymeric heterogeneous catalysts of transition-metal oxides. Figure 4 shows the XRD pattern of the polymeric catalyst based on copper oxide. The presence of three peaks centered at $\theta = 36.5, 39.7,$ and 49.8° confirms the presence of CuO in the studied catalyst. The XRD pattern of the polymeric multicomponent catalyst of transition-metal oxides, which consisted of 10 wt% MnO_2 , 2.5 wt% CuO, 2.5 wt% Co_3O_4 , 2.5 wt% Cr_2O_3 , 2.5 wt% NiO, and 80 wt% polyethylene,^[9] is shown in Figure 5. More characteristic peaks of metal oxides are shown in the diffractogram obtained for this catalyst. There is some evidence that the metal ions were always present on

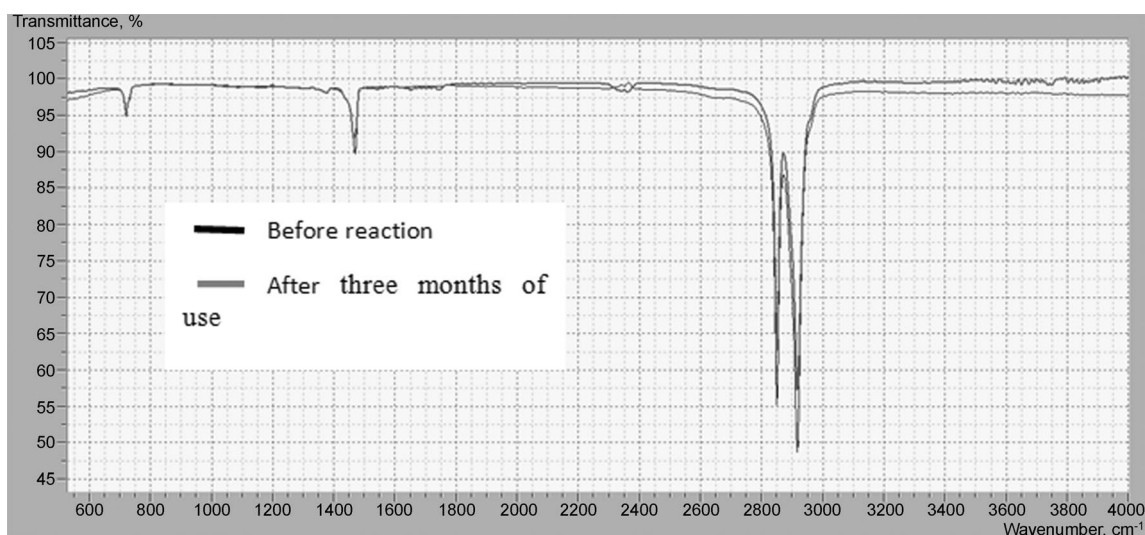


Figure 3. FTIR-spectra of MnO₂-10/CuO-10 before reaction and after three months of use.

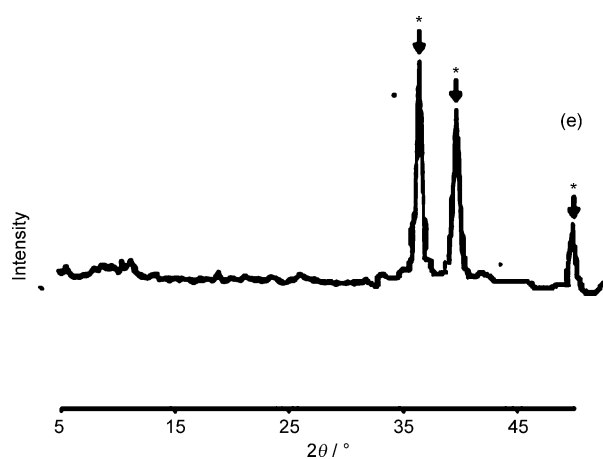


Figure 4. XRD pattern of the polymeric catalyst based on copper oxide.

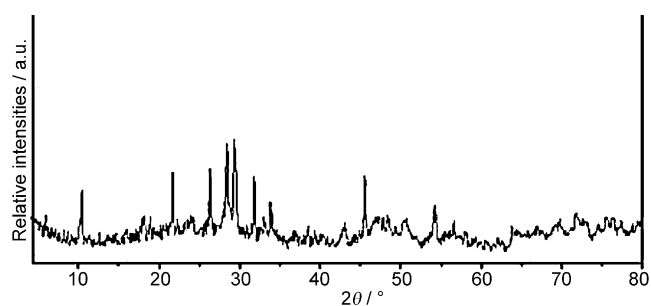


Figure 5. XRD pattern of the polymeric multicomponent catalyst of transition-metal oxides.

the catalyst surface, regardless of the elemental composition of the catalysts.

The surface morphology of the catalyst surface of MnO₂-10/CuO-10 was studied by using SEM under various magnifications (Figure 6). SEM is especially useful for examining the dis-

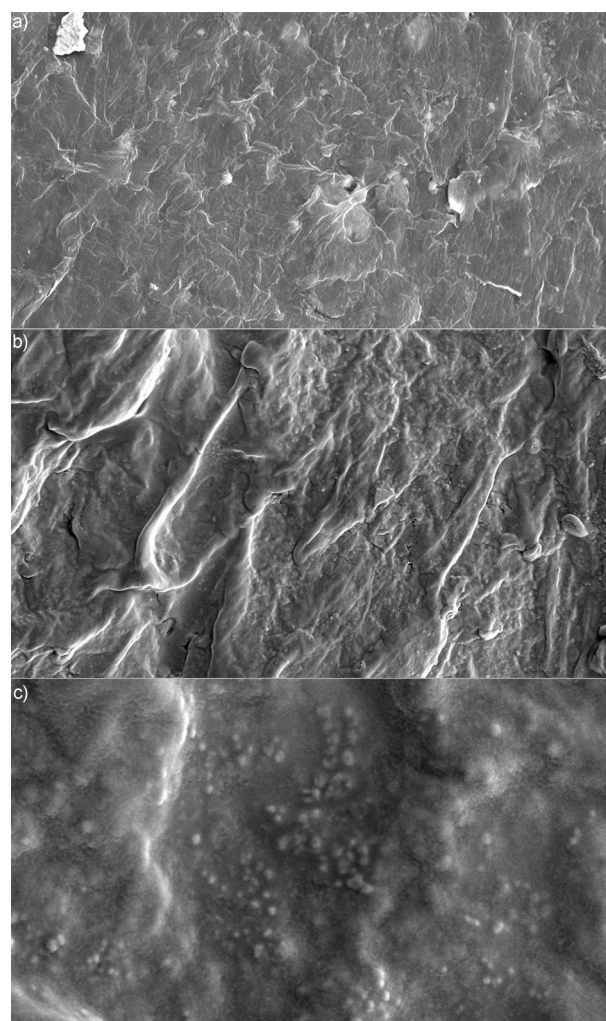
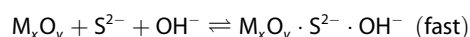


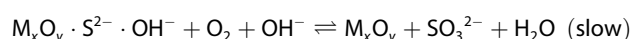
Figure 6. Surface morphology of the MnO₂-10/CuO-10 catalyst surface at various image magnifications: a) 500×, b) 5000×, and c) 25000×.

tribution and size of mesopores in such materials. According to Figure 6, the polymeric heterogeneous catalysts of transition-metal oxides do not have a highly porous structure, which is in good agreement with the low surface area and high stability of this sample. Transition-metal oxides were distributed evenly on the catalyst surface and were strongly adhered. Previous studies reported by our group^[9,20–24] indicated that the kinetics of the oxidation of sulfide ions in the presence of a polymeric heterogeneous catalyst of transition-metal oxides under alkaline conditions are zero-order with respect to sulfide concentration and first-order with respect to oxygen concentration. Thus, the following mechanism has been proposed:

Step 1 :



Step 2 :



This mechanism indicates the formation of complexes between transition-metal oxides and sulfide ions on the catalyst surface. Elemental analysis of the surface of the polymeric MnO₂-10/CuO-10 catalyst, before reaction and after three months of use, conducted by using SEM with an EDS detector,

revealed the absence of sulfide atoms in the elemental composition of the catalyst before reaction, but their presence after three months of use (see Figure 7 and Table 2). The elemental analysis also indicated no significant changes in the concentration of transition-metal oxides on the catalyst surface before reaction and after three months of use, providing good evidence that the catalyst surface is very stable under severe reaction conditions, which explains the retention of high catalytic activity for long-term use. It is important to note that the dis-

Table 2. Elemental composition of the polymeric MnO₂-10/CuO-10 catalyst sample.

Before reaction			After three months use		
element	[wt %]	[atom %]	element	[wt %]	[atom %]
C	91.28	95.72	C	90.94	95.58
O	4.09	3.22	O	4.04	3.19
Na	0.17	0.09	Na	0.11	0.06
Mn	2.64	0.60	Al	0.13	0.06
Cu	1.82	0.36	S	0.36	0.14
			Ca	0.11	0.04
Sum:	100.00	100.00	Mn	2.48	0.57
			Cu	1.83	0.36
			Sum:	100.00	100.00

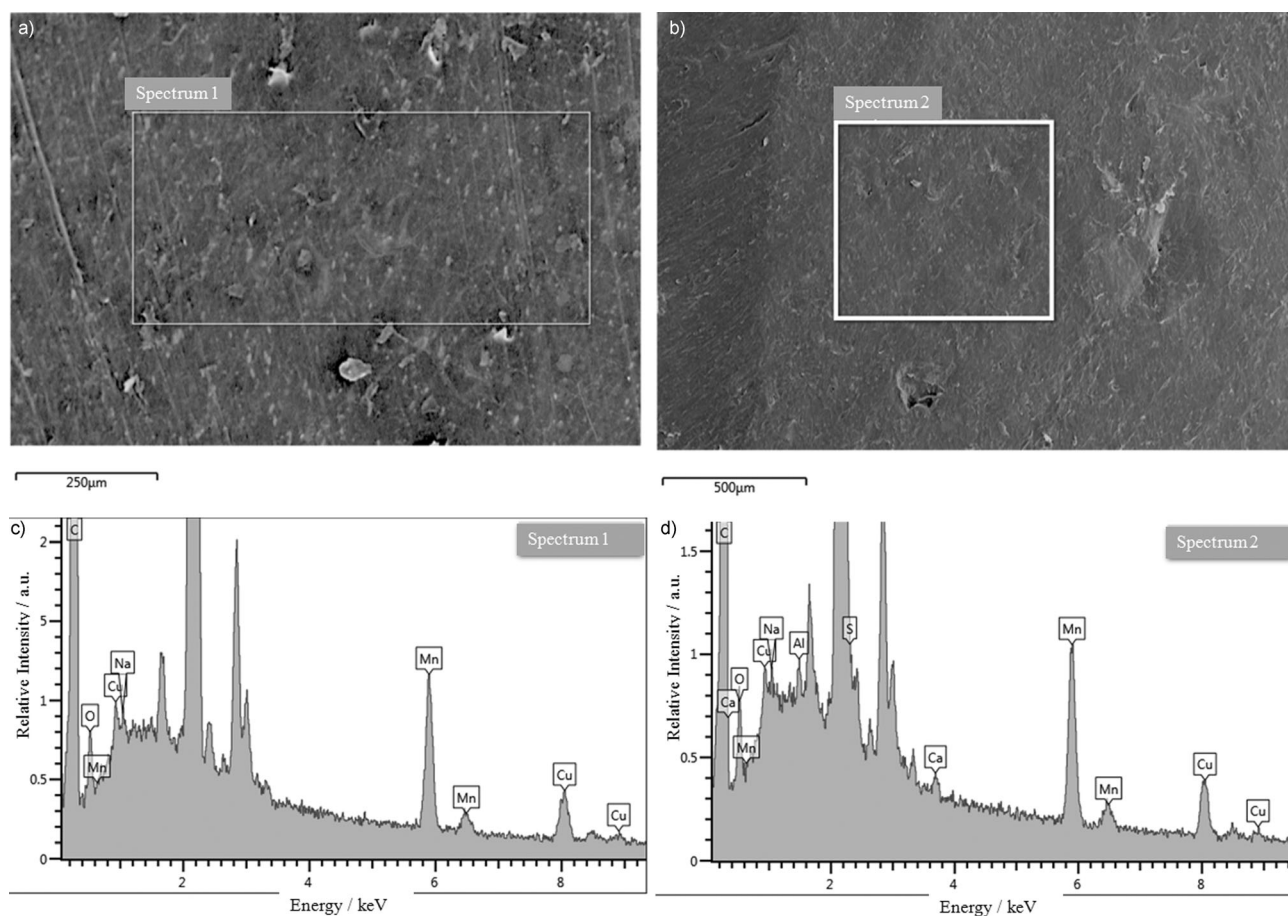


Figure 7. Backscattering SEM micrographs of the polymeric MnO₂-10/CuO-10 catalyst before reaction (a) and after three months of use (b). Corresponding EDS spectra before reaction (c) and after three months of use (d).

solution of transition-metal oxides of polymeric heterogeneous catalysts was not observed in the alkaline solution during the catalytic process, and so does not affect the catalytic reaction mechanism. Therefore, the application of these polymeric heterogeneous catalysts would not pose a threat to the environment and would provide a new technique for the removal of metal-oxide ions from wastewater.

As shown above, the formation of complexes between transition-metal oxides and sulfide ion occurs very quickly. These complexes are also unstable, quickly reacting with oxygen to form products. Therefore, elemental analysis only detected sulfide ions in regions with a high concentration of metal ions, which was confirmed by the backscattering SEM micrograph and the EDS spectrum of the polymeric $\text{MnO}_2\text{-10/CuO-10}$ catalyst obtained after three months of use at various locations on the catalyst surface (see Figure 8 and Table 3). Spectrum 3 was obtained from a region containing an Al impurity (Figure 8b).

Spectrum 3			Spectrum 4			Spectrum 5		
element	[wt%]	[atom%]	element	[wt%]	[atom%]	element	[wt%]	[atom%]
C	55.23	72.25	C	54.41	75.17	C	96.94	98.57
O	12.43	12.20	O	14.00	14.52	O	1.44	1.10
Al	22.05	12.84	S	4.49	2.32	Mn	0.80	0.18
Mn	4.39	1.25	K	0.25	0.11	Cu	0.81	0.16
Cu	5.91	1.46	Ca	0.94	0.39			
Sum:	100.00	100.00	Mn	17.67	5.34	Sum:	100.00	100.00
			Cu	8.23	2.15			
			Sum:	100.00	100.00			

The bright region (spectrum 4) is characterized by a high concentration of Cu and Mn ions (Figure 8c) as well as a high concentration of sulfide ions (Table 3). The dark region (spectrum 5) shows a low concentration of metal ions (Figure 8d) and there is a complete absence of sulfide ions (Table 3). In summary, the surface morphology of the catalyst and the distribution of the active phase strongly influence the activity of polymeric heterogeneous catalysts of transition-metal oxides.

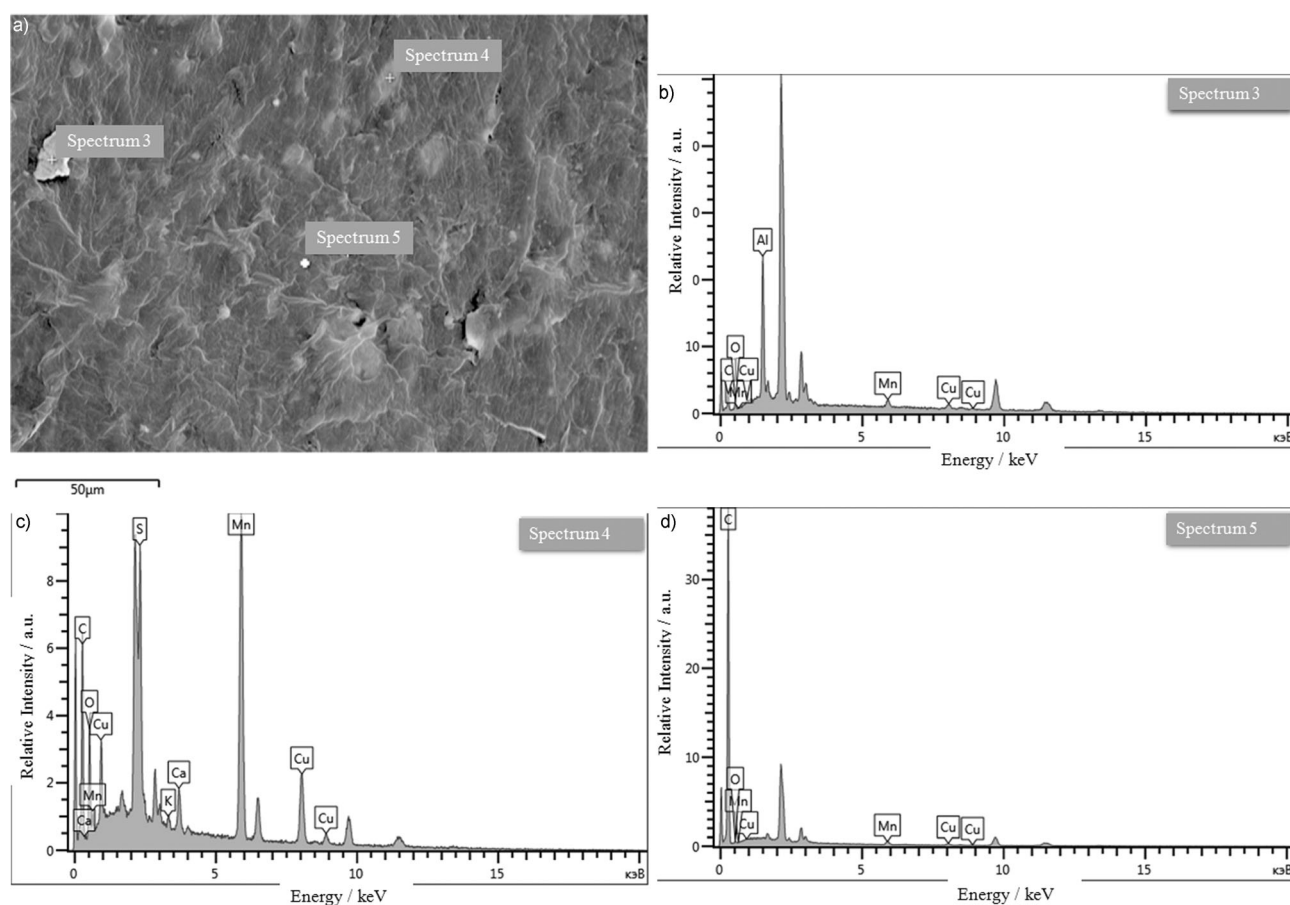


Figure 8. Surface of polymeric $\text{MnO}_2\text{-10/CuO-10}$ catalyst after three months of use: a) backscattering SEM micrograph, b) spectrum of a region with Al impurity (spectrum 3), c) spectrum of a bright region, indicating a high concentration of Cu and Mn ions (spectrum 4), and d) spectrum of a dark region, indicating a very low concentration of metal ions (spectrum 5).

Microstructural Characterization through X-ray-Computed Tomography

Particle-shape characterization is important when studying the behavior of a wide range of materials used in catalysis. X-ray-computed tomography provides high-resolution images of the internal structure of intact samples.^[31–36]

Although 2D measurements can be used to characterize and quantify morphological characteristics, only the spherical harmonic series, which are based on the images provided by 3D imaging techniques such as X-ray-computed tomography, can be used to reconstruct 3D particle profiles. Figure 9 shows the

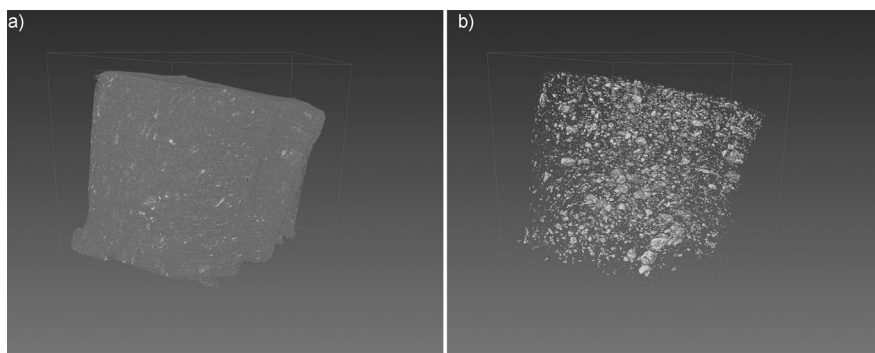


Figure 9. 3D structures of polymeric catalyst of transition-metal oxides obtained by using X-ray-computed tomography: a) external structure and b) internal structure after removing the polymeric layer.

3D structures of the polymeric heterogeneous catalysts of transition-metal oxides obtained by using X-ray-computed tomography. The 3D external structure is presented in Figure 9a, in which the metal ions are enclosed in the polymer matrix.

To obtain the crystalline structure of the metal ions, the polymer phase was removed (Figure 9b). According to Figure 10, the metal ions were distributed evenly and densely in the synthesized catalysts, which is important for regulating the catalytic activity by adjusting the catalyst size. Previous studies^[20,24] have reported that a change in the amount of polymeric heterogeneous catalyst incorporated (up to 5.0 g) had no influence on the reaction rate of the oxidation of sulfide and hydrosulfide ions.

The volume of the catalyst particles, which varied from 1.28×10^{-7} to $4.227 \times 10^{-3} \text{ mm}^3$, was also determined by using X-ray-computed tomography. A study of 280 132 particles found that most (92.9%) had

a small volume of $1.561 \times 10^{-6} \text{ mm}^3$, whereas the remaining particles ranged from 4.428×10^{-6} to $4.227 \times 10^{-3} \text{ mm}^3$ (Table 4). Investigators have recently generated high-quality images by using the local tomography variant of X-ray-computed tomography.^[37–40] Local tomography is achieved by scanning a sample larger than the field of view of the detector. Some parts of the sample are not observed by the detector for some values of the rotation angle. Provided that this missing information induces only a weak perturbation in a given measurement, reconstruction can be achieved successfully. Figure 11 shows an example of the reconstruction of the polymeric catalyst of transition-metal oxides examined in this

study, which indicates the presence of fine intermetallic particles and pores inside the solid phase, illustrating the ability of the imaging technique to resolve fine details in large samples.

Catalytic Activity

The oxidation rate induced by the heterogeneous multicomponent catalyst of transition-metal oxides (as stated above) in the oxidation of sulfur-containing compounds, including sodium sulfide (Na_2S), sodium hydrosulfide (NaSH), and sulfide ammonium ($(\text{NH}_4)_2\text{S}$), is compared with the rate induced by a heterogeneous transition-metal-oxide catalyst in polymeric phthalocyanine and the rate of non-catalyzed oxidation (Table 5). The experimental results indicate that

the rate induced by a heterogeneous transition-metal-oxide catalyst in polymeric phthalocyanine and the rate of non-catalyzed oxidation (Table 5). The experimental results indicate that

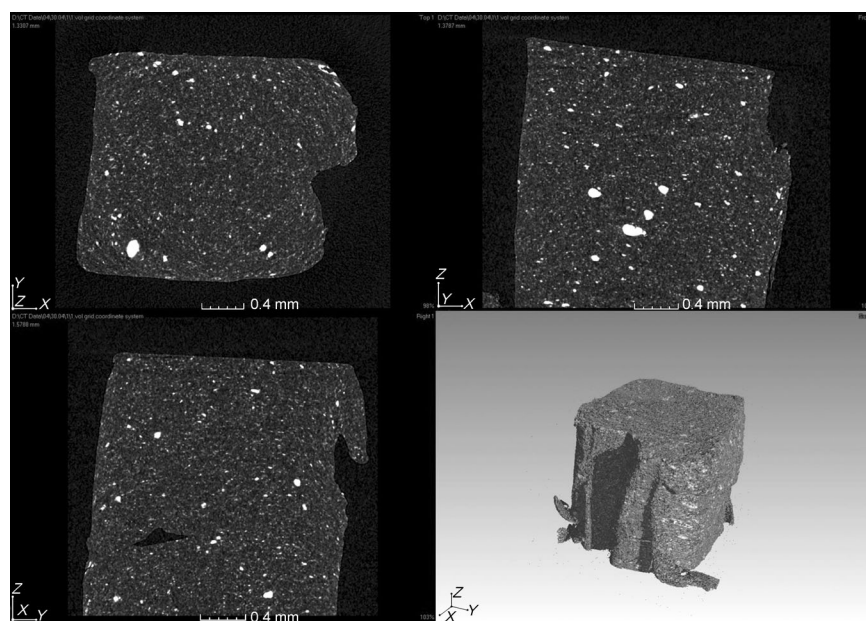
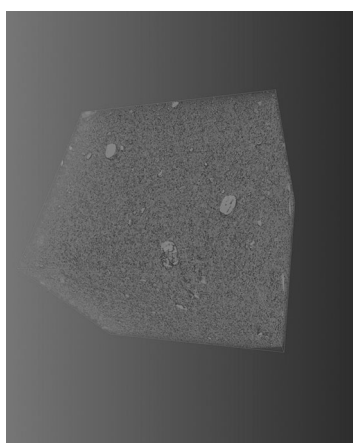


Figure 10. Cross-sections along the Z, X and, Y axes and 3D model of transition-metal oxides obtained by using X-ray-computed tomography.

Table 4. Particle distribution by volume.

Range number	Volume [mm ³]	Number of particles	Range number	Volume [mm ³]	Number of particles	Range number	Volume [mm ³]	Number of particles
1	1.5×10^{-6}	260305	11	3.0×10^{-5}	86	21	5.8×10^{-5}	22
2	4.4×10^{-6}	12736	12	3.3×10^{-5}	72	22	6.1×10^{-5}	16
3	7.2×10^{-6}	3205	13	3.5×10^{-5}	50	23	6.4×10^{-5}	19
4	1.0×10^{-5}	1277	14	3.8×10^{-5}	58	24	6.7×10^{-5}	25
5	1.3×10^{-5}	630	15	4.1×10^{-5}	43	25	7.0×10^{-5}	15
6	1.5×10^{-5}	397	16	4.4×10^{-5}	46	26	7.3×10^{-5}	7
7	1.8×10^{-5}	223	17	4.7×10^{-5}	32	27	7.6×10^{-5}	19
8	2.1×10^{-5}	180	18	5.0×10^{-5}	25	28	7.8×10^{-5}	11
9	2.4×10^{-5}	152	19	5.3×10^{-5}	27	29	8.1×10^{-5}	9
10	2.7×10^{-5}	115	20	5.6×10^{-5}	34	30–148	from 8.4×10^{-5} to 4.2×10^{-3}	296

**Figure 11.** Local tomography visualisation of the intermetallic particles inside a polymeric catalyst of transition-metal oxides.**Table 5.** Initial oxidation rate of sulfur-containing compounds in the presence of various catalysts. Initial concentration $C_0 = 0.4 \text{ g L}^{-1}$, oxidation time $t = 60 \text{ min}$, conversion = 99.99%.

S compound	Initial oxidation rate [$\text{mg L}^{-1} \text{c}^{-1}$]		
	non-catalyzed oxidation	polymeric catalyst	multicomponent catalyst
Na_2S	0.67	1.26	2.23
NaSH	0.71	1.35	2.49
$(\text{NH}_4)_2\text{S}$	1.36	1.94	3.69

the heterogeneous multicomponent catalyst exhibited high activity in the oxidation of all sulfur-containing compounds. Specifically, the oxidation catalyzed by the heterogeneous multicomponent catalyst showed initial rates approximately 1.7, 1.8, and 1.9 times higher than those of the commercial catalyst, and 3.3, 3.5, and 2.9 times higher than the non-catalyzed reaction for Na_2S , NaSH and $(\text{NH}_4)_2\text{S}$, respectively.

3. Conclusions

The physicochemical properties of polymeric heterogeneous catalysts of transition-metal oxides, including the specific surface area, elongation at break, breaking strength, specific elec-

trical resistance, and volume resistivity were studied. Although these catalysts possessed a low surface area, they were stable under severe reaction conditions. Morphological and elemental analyses of the polymeric catalyst surfaces were conducted by using digital microscopy, FTIR spectroscopy, XRD, SEM, and EDS. The catalyst surface did not change after three months of use under relatively severe reaction conditions (60°C , 5.0% alkaline concentration, and $1400 \text{ rev min}^{-1}$ solution rotational speed). XRD analysis revealed the presence of metal ions on the catalyst surface. SEM and elemental analysis also indicated that there was no dissolution of the transition-metal oxides of the polymeric heterogeneous catalysts in the alkaline solution during the catalytic process, and the sulfide ions were only detected in regions with high concentrations of metal ions. These results confirmed the oxidation mechanism of sulfur-containing compounds in the presence of polymeric heterogeneous catalysts of transition-metal oxides reported in our previous papers. Microstructural characterization of the polymeric heterogeneous catalyst of transition-metal oxides was performed by using X-ray-computed tomography, which indicated that the metal ions were distributed evenly and densely throughout the synthesized catalysts. The activities of the various catalysts in the oxidation of sulfur-containing compounds were determined. In summary, polymeric heterogeneous catalysts of transition-metal oxides possess desirable properties and can be applied for industrial wastewater treatment.

Keywords: electron microscopy · heterogeneous catalysis · IR spectroscopy · sulfur · transition metals

- [1] F. E. Hancock, *Catal. Today* **1999**, *53*, 3–9.
- [2] I. Zermeno-Montante, C. Nieto-Delgado, R. D. Sagredo-Puente, M. G. Cárdenas-Galindo, B. E. Handy, *Top. Catal.* **2011**, *54*, 579–586.
- [3] A. B. Sorokin, *Chem. Rev.* **2013**, *113*, 8152–8191.
- [4] B. Basu, S. Satapathy, A. K. Bhatnagar, *Catal. Rev. Sci. Eng.* **1993**, *35*, 571–609.
- [5] R. M. Ahmadullin, A. G. Ahmadullina, S. I. Agadjanyan, A. R. Zaripova, *Refin. Petrochem.* **2012**, *6*, 10–16.
- [6] A. G. Ahmadullina, R. M. Ahmadullin, *Chem. Technol Fuels Oils* **2008**, *44*, 371–378.
- [7] A. G. Ahmadullina, B. V. Kizhaev, G. M. Nurgalieva, A. S. Shabaeva, S. O. Tugushi, N. V. Haritonov, *Refin. Petrochem.* **1994**, *2*, 39–42.
- [8] A. G. Ahmadullina, A. S. Shabaeva, G. M. Nurgalieva, RU patent 2053844, **1996**.

- [9] B. D. Nhi, R. M. Ahmadullin, A. G. Ahmadullina, S. I. Aghajanian, *J. Sulfur Chem.* **2013**, DOI: 10.1080/17415993.2013.800062.
- [10] A. B. Kilimnik, *Tambov: Thumb. State. tehn. Univ.* **2008**, *1*, 1–96.
- [11] L. Lung-Chang, L. Chung-Chun, T. H. Andrew, *J. Porphyrins Phthalocyanines* **2001**, *5*, 806–807.
- [12] J. Yang, PhD thesis, Dublin City University (Ireland), **2006**.
- [13] H. Wang, X. Z. Liao, Q. Z. Jiang, X. W. Yang, Y. S. He, Z. F. Ma, *Chin. Sci. Bull.* **2012**, *57*, 1959–1963.
- [14] V. I. Marshneva, V. V. Mokrinskii, K. A. Dubkov, *Mechanism and Kinetic, 1st European Congr. Catal.*, Montpellier, France, **1993**, p. 4.
- [15] R. L. Huang, J. H. Espenson, *J. Mol. Catal., A* **2001**, *168*, 39–46.
- [16] R. Aldea, H. Alper, *J. Org. Chem.* **1995**, *60*, 8365–8366.
- [17] X. T. Zhou, H. B. Ji, Z. Cheng, J. C. Xu, L. X. Pei, L. F. Wang, *Bioorg. Med. Chem. Lett.* **2007**, *17*, 4650–4653.
- [18] E. Boring, Y. V. Geletii, C. L. Hill, *J. Am. Chem. Soc.* **2001**, *123*, 1625–1635.
- [19] H. Zhang, C. Y. Chen, R. H. Liu, Q. Xu, W. Q. Zhao, *Molecules* **2010**, *15*, 83–92.
- [20] B. D. Nhi, R. M. Ahmadullin, A. G. Ahmadullina, I. D. Samuilov, *Kazan State Technological University Bulletin* **2012**, *15*, 50–54.
- [21] B. D. Nhi, R. M. Ahmadullin, A. G. Ahmadullina, *Butlerov Commun.* **2012**, *30*, 94–97.
- [22] B. D. Nhi, R. M. Ahmadullin, A. G. Ahmadullina, *Butlerov Commun.* **2012**, *32*, 155–158.
- [23] B. D. Nhi, R. M. Ahmadullin, A. G. Ahmadullina, I. D. Samuilov, *Kinet. Catal.* **2013**, *54*, 334–337.
- [24] B. D. Nhi, R. M. Ahmadullin, A. G. Ahmadullina, I. D. Samuilov, *Tap Chi Hoa Hoc (Vietnam)*, **2012**, *50*, 219–222.
- [25] A. M. Mazgarov, A. F. Vildanov, I. Arhireeva, O. A. Olga, N. R. Aiupova, RU patent 1041142, **1983**.
- [26] A. G. Akhmadullina, RU GOST 22985–90, **1991**.
- [27] Y. Y. Lurie, *Analytical Chemistry of Industrial Waste water*, Khimiya, Moscow, **1984**, p. 330.
- [28] S. Lowell, S. Sielids, *Powder Surface Area and Porosity*, Chapman and Hall, London, **1991**, pp. 11–26.
- [29] M. Marzantowicz, J. R. Dygas, F. Krok, E. ZygadLo-Monikowska, Z. Florjanczyk, *Mater. Sci. Poland* **2006**, *24*, 195–203.
- [30] H. Chen, H. Tao, Q. Wu, X. Zhao, *J. Am. Ceram. Soc.* **2013**, *96*, 801–805.
- [31] P. J. Withers, M. Preuss, *Annu. Rev. Mater. Res.* **2012**, *42*, 81–103.
- [32] G. Requena, H. P. Degischer, *Annu. Rev. Mater. Res.* **2012**, *42*, 145–161.
- [33] M. Eric, *Annu. Rev. Mater. Res.* **2012**, *42*, 163–178.
- [34] J. K. Torrance, T. Elliot, R. Martin, R. J. Heck, *Cold Reg. Sci. Technol.* **2008**, *53*, 75–82.
- [35] L. About, E. Maire, J. Y. Buffière, R. Fougères, *Acta Mater.* **2001**, *49*, 2055–2063.
- [36] E. Masad, S. Saadeh, T. Al-Rousan, E. Garboczi, D. Little, *J. Comput. Mater. Sci.* **2005**, *34*, 406–424.
- [37] A. Faridani, K. A. Buglione, P. Huabsomboon, O. D. Iancu, J. McGrath, *Contemp. Math.* **2001**, *278*, 29–47.
- [38] E. L. Ritman, S. M. Jorgensen, P. E. Lund, P. J. Thomas, J. H. Dunsmuir, *Proc. SPIE* **1997**, *3149*, 13–24.
- [39] S. Bonnet, F. Peyrin, F. Turjman, R. Prost, *IEEE Trans. Image Process.* **2000**, *9*, 1445–1450.
- [40] H. Toda, T. Ohgaki, K. Uesugi, K. Makii, Y. Aruga, *Key Eng. Mater.* **2005**, *297*, 1189–1195.

Received: August 8, 2013

Revised: September 16, 2013

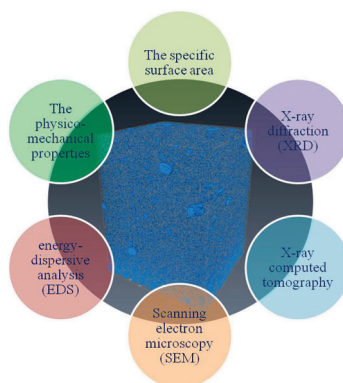
Published online on ■ ■ ■, 2013

ARTICLES

B. D. Nhi,* R. M. Akhmadullin,
A. G. Akhmadullina, Y. D. Samuilov,
S. I. Aghajanian



Polymeric Heterogeneous Catalysts of Transition-Metal Oxides: Surface Characterization, Physicomechanical Properties, and Catalytic Activity



Analysis of catalyst: Various modeling techniques and methodologies are used to characterize the surface and to study the physicomechanical properties and activity of polymeric heterogeneous catalysts of transition-metal oxides. The experimental results indicate that the investigated catalysts can be applied for industrial wastewater treatment.